Journal of Chromatography, 638 (1993) 215–223
Elsevier Science Publishers B.V., Amsterdam

CHROM. 24 922

Study of isotachophoretic separation behaviour of metal cations by means of particle-induced X-ray emission

V. Fractionation of platinum group elements from a model solution of nuclear fuel waste by means of continuous free-flow isotachophoresis

Takeshi Hirokawa*, Takao Ohta, Isamu Tanaka, Ken-ichiro Nakamura, Wen Xia, Fumitaka Nishiyama and Yoshiyuki Kiso☆

Applied Physics and Chemistry, Faculty of Engineering, Hiroshima University, Kagamiyama 1, Higashi-hiroshima 724 (Japan)

ABSTRACT

The fractionation of platinum group elements from a model solution of a high-level liquid waste was investigated using a continuous free-flow isotachophoretic analyser. The leading electrolytes used contained α-hydroxyisobutyric acid (HIB) and tartaric acid as the complex-forming agent, where 20 m*M* NH_4^+ was the leading ion and acetic acid was the pH buffer (pH 4.8). The fractions were analysed off-line by means of particle-induced X-ray emission (PIXE). It was found that Fe and platinum group elements split into two zones of cations and non-ions when HIB was used, but all of them was recovered as non-ions when tartaric acid was used. In both electrolyte systems, 100% recovery as cations was obtained for Cs^+, Rb^+, Ba^{2+}, Sr^{2+}, Na^+, Cr^{2+}, Mn^{2+}, Ni^{2+}, La^{3+}, Ce^{3+}, Pr^{3+}, Nd^{3+}, Sm^{3+}, Eu^{3+}, Gd^{3+} and Y^{3+}. It was concluded that free-flow isotachophoresis would be very useful for fractionating platinum group elements from other metal ions.

INTRODUCTION

In the preceding paper [1] we reported the isotachophoretic (ITP) separation behaviour of a model mixture of a high-level liquid waste (HLLW) by the use of a capillary-type isotachophoretic analyser [1]. An HLLW is generated in the reprocessing stage of a nuclear fuel cycle to recover Pu and U and it contains 30 or more elements: the constituents are the fission products of U (light lanthanides, Cs, Sr and platinum group elements), the fuel cladding materials (Zr) and solidifying agent ($NaNO_3$). An actual HLLW contains considerable amounts of platinum group metals, such as palladium, which have very low radioactivity and may be useful as a catalyst material. For this purpose, they must be separated from the co-existing long-lived and highly radioactive nuclides such as Cs and Sr.

In order to clarify the possibility of using ITP as a fractionating method for HLLW, in this work the separation behaviour of platinum group elements in a model HLLW was investigated by the use of a continuous free-flow ITP apparatus. The fractions were analysed off-line by particle-induced X-ray emission (PIXE). Two kinds of

* Corresponding author.
☆ Present address: Hijiyama Women's College, Ushita-shin-machi, Hiroshima, 732, Japan.

0021-9673/93/$06.00

complex-forming agents, α-hydroxyisobutyric acid and tartaric acid, were used. The recovery of the components, migration order and separation efficiency of the HLLW components are reported.

THEORETICAL

Processing ability of a free-flow isotachophoretic instrument

In capillary ITP, the boundary velocity at the steady state remains constant with time provided that a constant current is supplied. However, in free-flow ITP, the boundary velocity decreases during the transit time, even if the migration current is kept constant, because the distribution of migration current in the separation chamber is not homogeneous, that is, the current density decreases from the sample inlet to the outlet with the development of the ITP terminating zone.

Apart from the above point, there is no fundamental difference between capillary ITP and continuous free-flow ITP. The amount of sample separable depends on the amount of electricity during the migration process [2,3]. In the actual instrument, the suppliable amount of electricity depends linearly on the load of the leading electrolyte [2,3]; to increase the load to a capillary ITP analyser, it is necessary to use a long separation tube and/or a concentrated leading electrolyte. Similarly, the separability of a free-flow ITP instrument depends on the volume of the separation chamber occupied by the leading electrolyte and the concentration of the electrolyte.

The separable sample amount (SA) of a free-flow ITP analyser during the transit time [t (s)] may consist of three factors:

$$SA = SIt \quad (1)$$

where S denotes the separability of the sample (mol/C) under the electrolyte system and I is the migration current (A). The current I may be set so as not to generate an excess migration voltage, *i.e.*, to keep the target zones within the fractions. Therefore, the current I is closely related to the flow-rate of the electrolyte in the sample chamber. If a high flow-rate is necessary to reduce the transit time, a high migration current can be applied within the practical limit of the cooling unit used. If a long transit time is allowed, the migration current must be set low to prevent overmigration. Consequently, the amount of electricity (Q) is automatically determined by the volume of the separation chamber occupied by the leading electrolyte.

In principle, the separability S is the same as in capillary ITP, provided that the same electrolyte system is used at the same temperature.

The processing ability (P) of the apparatus per unit time (mol/h) can be defined as

$$P = SI \cdot 3600 \quad (2)$$

The actual sampling rate must be smaller than P. It should be noted that the sum of the zone lengths of the sample components cannot exceed the effective width of the sample chamber.

Hence the processing ability of a free-flow ITP instrument for a sample can be estimated from the separability of a capillary ITP analyser.

EXPERIMENTAL

Samples

A non-radioactive model solution of HLLW (MW-2), which contained 27 kinds of metal ions, was used as the sample [1]. The composition of MW-2 was simulated by Power Reactor and Nuclear Fuel Development (Tokyo, Japan). As the original solution was strongly acidic (2.5 mol/l nitric acid solution), it was not suitable as the sample for ITP. Therefore, the solution was dried to remove nitric acid using an evaporator, and the residue was dissolved by adding deionized water. This process was repeated three times. The solution obtained (pH ≈ 1.5) was diluted with deionized water to 1/350 of the concentration of the original solution. The solution obtained (pH 3.2) was used as the sample. The component concentrations are given in Table I. Small amounts of cationic dyes, toluidine blue (TB) and astrazon pink (AP), were added to the above sample in order to monitor the positions of the zones.

TABLE I

CONCENTRATIONS OF COMPONENTS OF THE MODEL WASTE MW-2

Z	Element	Form[a]	Concentration (μM)	Z	Element	Form	Concentration (μM)
11	Na	$NaNO_3$	2802.9	46	Pd	$Pd(NO_3)_2$	24.74
13	Al	Al	0.13	47	Ag	$AgNO_3$	1.00
15	P	P	36.3	48	Cd	$Cd(NO_3)_2$	1.40
24	Cr	$Cr(NO_3)_3$	11.29	50	Sn	Sn	0.94
25	Mn	$Mn(NO_3)_2$	37.46	52	Te	TeO_2	10.20
26	Fe	$Fe(NO_3)_3$	222.0	55	Cs	$CsNO_3$	46.00
28	Ni	$Ni(NO_3)_2$	26.77	56	Ba	$Ba(NO_3)_2$	27.77
34	Se	Na_2SeO_3	1.54	57	La	$La_2(CO_3)_3$	23.46
37	Rb	$RbNO_3$	10.40	58	Ce	$Ce(CO_3)_2$	168.3
38	Sr	$Sr(NO_3)_2$	25.09	59	Pr	Pr_6O_{11}	21.31
39	Y	Y_2O_3	13.91	60	Nd	Nd_2O_3	71.43
40	Zr	$ZrO(NO_3)_2$	103.1	62	Sm	Sm_2O_3	14.57
42	Mo	Na_2MoO_4	87.43	63	Eu	Eu_2O_3	2.29
44	Ru	$Ru(NO_3)_3$	48.29	64	Gd	Gd_2O_3	1.11
45	Rh	$Rh(NO_3)_3$	9.69	72	U	$UO_2(NO_3)_2$	12.13

[a] Chemical forms of the reagents used.

Electrolyte system

Two leading electrolytes were used, as shown in Table II. One was 20 mM ammonia solution containing 10 mM α-hydroxyisobutyric acid (HIB) as the complex-forming agent. The pH of the leading electrolyte (pH_L) was adjusted to 4.8 by adding acetic acid. This system is referred to as WNH_4Ac–HIB. The other was 20 mM ammonia solution containing 1 or 2 mM tartaric acid as the complex-forming agent. The pH of the leading electrolyte (pH_L) was adjusted to 4.8 also by adding acetic acid. This system is referred to as WNH_4Ac–Tar. Hydroxypropylcellulose (HPC) was added to both leading electrolytes (0.1%, w/w) to suppress electroosmotic flow. The terminating electrolyte used was 10 mM carnitine hydrochloride for both leading electrolytes.

The operational electrolyte systems used permits two-dimensional isotachophoresis [4,5], *i.e.*, both cations and anions can migrate isotachophoretically toward the respective electrodes. The leading anion was 10 mM Cl^- and the terminating ion was 10 mM HIB or 1 mM Tar.

All the reagents used were purchased from

TABLE II

ELECTROLYTE SYSTEMS USED IN ISOTACHOPHORETIC SEPARATIONS

HIB = α-hydroxyisobutyric acid; Tar = tartaric acid; HPC = hydroxypropylcellulose.

Parameter	WNH_4Ac–HIB	WNH_4Ac–Tar
Leading electrolyte	20 mM NH_3 solution	20 mM NH_3 solution
Complexing agent	10 mM HIB	1 mM Tar
pH buffer	Acetic acid	Acetic acid
pH	4.80	5.00
Additive	0.1% HPC	0.1% HPC
Terminating electrolyte	10 mM carnitine hydrochloride	
pH	2.5	

Tokyo Kasei (Tokyo, Japan). pH measurements were carried out using a Horiba (Tokyo, Japan) Model F7ss expanded pH meter.

Free-flow isotachophoretic instrument

The preparative instrument used was a Bender and Hobein Elphor Vap 22. Fig. 1 illustrates the electrolyte circuits of the apparatus when it was operated in the ITP mode. The effective size of the separation chamber (SC) was 10 cm wide, 50 cm high and 0.5 mm thick. The sample solution (S) was supplied by a sixfold peristaltic pump (P1) together with the leading electrolyte (L2) and the terminating electrolyte (T2). Ninety fractions were obtained using a 90-fold peristaltic pump (P2). The leading and terminating electrolytes (L1 and T1) used for the electrode compartments (L and T) were 2 l in volume and they were circulated by pumps (PL and PT) during migration. The separation chamber was thermostated at 15°C.

PIXE analysis

For the measurement of PIXE spectra, a Model AN-2500 Van de Graaff accelerator (Nisshin High Voltage, Tokyo, Japan) at the Faculty of Engineering, Hiroshima University, was used. The energy of the H^+ beam was 2.0 MeV and the beam current was 20–50 nA. A typical single run for ITP fractions took 190–260 s. The detector used was a high-purity Ge detector (ORTEC Model GLP-10180) and the multi-channel analyser used was a Laboratory Equipment (Tokyo, Japan) Model AMS-1000.

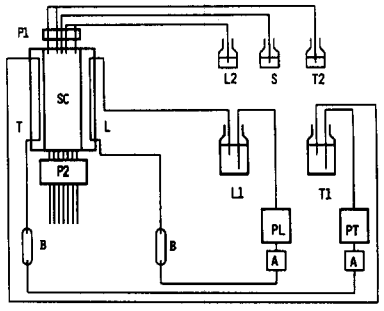

Fig. 1. Electrolyte circuits of free-flow isotachophoresis instrument. SC = separation chamber; L = leading electrolyte and electrode compartment; T = terminating electrolyte and electrode compartment; P1 = peristaltic pump to feed sample and electrolyte; P2 = 90-fold peristaltic pump for fractionation; S = sample solution reservoir; L1 and L2 = leading electrolyte reservoir; T1 and T2 = terminating electrolyte reservoir; PL and PT = electrolyte circulation pumps; A = flow-rate adjuster; B = bubble trap.

The Nuclepore filter used as the target backing material was of thickness 5 μm and pore size 0.1 μm, and was mounted on an aluminium flame. Each fraction was sampled using a 5-μl pipette (Eppendorf Model 4700) on to the filter. The diameter of the fraction spot was *ca.* 3 mm. A PIXE spectrum was measured for each fraction after drying in a desiccator. In order to calibrate the PIXE sensitivities, standard samples (5 μl, 1000 ppm solution for atomic absorption spectrometry; Tokyo Kasei) were used.

A few or more components were contained in a fraction when the abundances were low. The computer code PIXS developed previously [6] was used to analyse the PIXE spectra. Least-squares fitting for spectrum deconvolution was carried out utilizing the X-ray relative intensity database, which was optimized to our measurement system. Calculations were carried on an NEC (Tokyo, Japan) PC-9801RA microcomputer (CPU = 80 386, co-processor = 80 387, clock = 20 MHz). It took 1 min to analyse the spectrum of one fraction.

RESULTS AND DISCUSSION

Determination of sample rate

As the present sample was inorganic, a longer transit time caused no problems. We selected the minimum value appropriately as *ca.* 500 s. In the actual experiments, the transit time was calculated from the flow-rate and the volume of the sample chamber ($10 \times 50 \times 0.25$ cm) and the sample flow-rate was adjusted to give a residence time of 500 s. The total flow-rates of the leading electrolyte, terminating electrolyte and the sample solution were 191.4, 125 and 96 ml/h, respectively. The electrolytes were supplied to the separation chamber by a sixfold peristaltic pump, where one port was for the sample solution, three ports were for the leading electrolyte and two ports were for the terminating electrolyte. The same transit times were calculated as 471, 720 and 937 s, respectively, and the migration current I was fixed at 30 mA.

Capillary ITP experiments have shown that the separability of MW-2 using the WNH_4Ac–HIB system was 1.14 μmol/C at 25°C [1]. From this value and the migration current, the processing ability (P in eqn. 2) can be calculated as 123 μmol/h. To achieve this value at a flow-rate of 31.9 ml/h, the original model solution was diluted 1:350. Therefore, the molar sampling rates at the other flow-rates were 80 and 60 μmol/h.

Separation behaviour of MW-2 with the WNH_4Ac–HIB system

The migration order of MW-2 components using the WNH_4Ac–HIB system was ascertained from capillary ITP experiments to be Cs^+, Rb^+, Ba^{2+}, Sr^{2+}, Na^+, Mn^{2+}, Fe^{2+}, (Cr^{2+}, Rh^{2+}, Cd^{2+}), Ni^{2+}, La^{3+}, Ce^{3+}, Pr^{3+}, Nd^{3+}, Sm^{3+}, Eu^{3+}, Gd^{3+}, Y^{3+}, (Fe^{3+}, Ru^{3+}, Rh^{3+}, ZrO^{2+}). It should be noted that mobilities of Cs^+ and Rb^+ are larger than that of the leading ion NH_4^+ and therefore these ions migrate zone electrophoretically in the leading zone. A concentrated colloidal zone containing Fe, Ru, Rh and ZrO was observed just before the terminating zone. Although the cation recovery was 100% for Ba^{2+}, Sr^{2+}, Na^+, (Cd^{2+}, Cr^{2+}), Ni^{2+}, La^{3+}, Ce^{3+}, Pr^{3+}, Nd^{3+}, Sm^{3+}, Eu^{3+}, Gd^{3+} and Y^{3+}, almost all of Fe^{3+}, Ru^{3+} and Rh^{3+} and half of ZrO^{2+} and Rh^{2+} could not be recovered as cations. The components migrating as anions were a part of MoO_4, Zr and Se. The low cation recovery of Fe^{3+}, Ru^{3+}, Pd^{3+} and Rh^{3+} suggested that the remainder might form immobile non-ions [1,7].

Fig. 2 shows the results of PIXE analysis for each of the fractions that were obtained with the continuous free-flow instrument varying the sampling rate of MW-2 at (A) 123, (B) 80 and (C) 60 μmol/h. Not all of the fractions were analysed. The sample injection port used was positioned approximately above the 55th fractionating port. Although the electrolyte system used permits two-dimensional ITP, the anionic components were not fractionated because of the small width (10 cm) of the separation chamber used and the low abundances [1]. The sample components shown in Fig. 2 were restricted to the representative components Fe, Ce, Ba, Cs and platinum metals. The distribution of Na was not determined (PIXE inactive) but it has already been found in experiments using capillary ITP that an Na zone existed between the Ba and Ce zones [1].

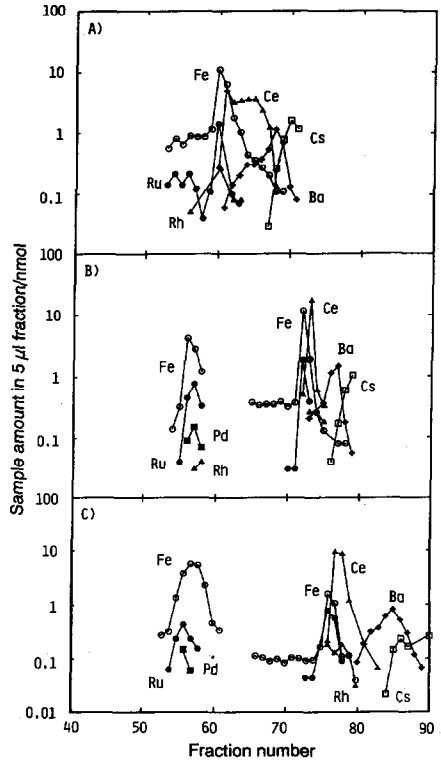

Fig. 2. Analytical results for the cationic and non-ionic fractions of MW-2 obtained by means of PIXE with the WNH_4Ac–HIB system. The molar sampling rate was (A) 123, (B) 80 and (C) 60 μmol/h. For the electrolyte system, see Table II; migration current = 30 mA; temperature of separation chamber = 15°C.

Apparently from Fig. 2, the separability depended on the sampling rate. In fact, we could observe the separation process of the MW-2 components by changing the sampling rate. At 123 μmol/h the separation was in the initial stage, and at 60 μmol/h the separation was still incomplete. Better results will be obtained at the lower sampling rate, although the present experiments gave enough information on the separation behaviour of MW-2. The actual processing ability was thus smaller than that calculated from capillary ITP experiments, which might be main-

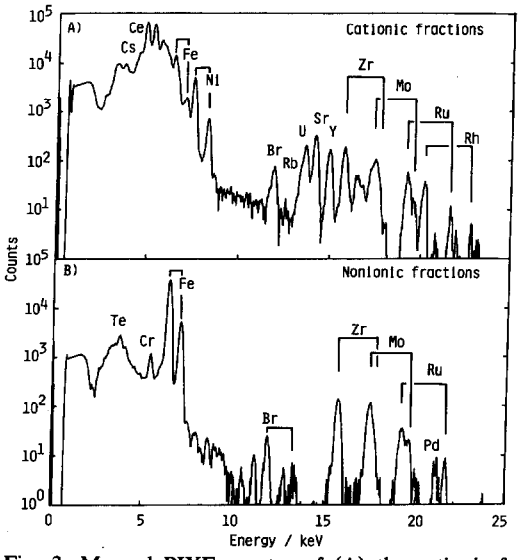

Fig. 3. Merged PIXE spectra of (A) the cationic fractions and (B) the non-ionic fractions. Electrolyte system, WNH_4Ac–HIB; $E_p = 2$ MeV.

ly due to the fact that the temperature of the separation chamber was thermostated at 15°C.

Fig. 3 shows the merged PIXE spectra of the cationic fractions and non-ionic fractions. Obviously from Fig. 3, Fe, Zr, Mo and platinum group elements (Ru, Rh and Pd) split into two zones of non-ions and cations. This is the significant feature of the separation behaviour when this electrolyte system is used.

Table III summarizes the component amounts determined by PIXE together with the cation and anion recoveries. Most of the component amounts agreed with each other within experimental errors. The significant decrease in the Cs and Rb levels was due to the fact that not all of the zones were analysed and at the lowest sampling rate (Fig. 2C) the Cs and Rb zones migrated into the leading electrode compartment.

In Fig. 2B, the Fe zone shows a long tail. This suggested that the colloidal Fe zone migrating just before the terminating zone was not stable and the amount of Fe in the Fe zone decreased gradually during migration. Table IV gives the relative abundances of MW-2 components in the original sample and the fractions where Ce was normalized as 100. The abundance of Fe non-ions and Fe cations were 86% and 14% at 123 μmol/h and 17% and 83% at 60 μmol/h, respectively. A similar change was observed for platinum group elements, although not as large. Moreover, the total amount of Fe decreased slightly.

This observation was not an experimental error, as we observed the formation of a red-brown precipitate of Fe compounds in the separation chamber as a narrow stream with 60 μmol/h operation, and the precipitate was found at the bottom of the fractions tubes which corresponded to the non-ions.

The relative abundances of the components agreed well with each other among three experiments, as shown in Table IV. However, in comparison with the relative abundance of the sample, significant differences were found for Zr, Mo, Ru, Rh and Pd, suggesting that these were not contained in the sample solution. In fact, the original sample was the filtered solution of the original mixture. Insoluble substances consisted mainly of Zr. Small amounts of Mo, Ru, Rh, Pd and other elements were also found in the precipitate.

Separation behaviour of MW-2 with the WNH_4Ac–Tar system

Fig. 4 shows the analytical results for the fractions. Although the separation behaviour was very similar to that for the WNH_4Ac–HIB system for many components, very different separation behaviour was observed for Fe, Zr, Mo and platinum group elements, *i.e.*, the Fe, Zr and Mo zones migrating just before the terminating electrolyte observed with the WNH_4Ac–HIB system disappeared completely. Most of Fe was found as non-ions and only a small amount was fractionated at Fe^{2+}.

Fig. 5 shows the merged PIXE spectra of the cationic and non-ionic fractions. The above discussion about the migration behaviour of Fe, Zr and Mo is obvious from Figs. 3 and 5. That is, the X-ray bands of Fe, Zr and Mo were significant in Fig. 3A but not in Fig. 5A. One more important observation was that the UO_2^{2+} ion was not observed in the cationic fractions with the WNH_4Ac–Tar system, because the effective mobility of UO_2^{2+} with the WNH_4Ac–Tar system

TABLE III

SAMPLE AMOUNTS IN FRACTIONS ANALYSED BY PIXE

Electrolyte system: WNH_4Ac–HIB. T = total amount (nmol) of sample components found in 5-μl fractions; C = recovery as cations (%); N = recovery as non-ions (%).

Z	Element	Sampling rate (μmol/h)								
		123			80			60		
		T (nmol)	C (%)	N (%)	T (nmol)	C (%)	N (%)	T (nmol)	C (%)	N (%)
24	Cr	1.36	100	0	1.30	92	8	0.76	100	0
25	Mn	5.30	100	0	4.70	100	0	4.56	100	0
26	Fe	28.64	86	14	27.22	67	33	23.02	17	83
28	Ni	3.61	100	0	3.30	100	0	3.02	100	0
34	Se	nd[a]								
37	Rb	0.96	100	0	0.44	100	0	0.07	100	0
38	Sr	2.94	100	0	2.92	100	0	2.76	100	0
39	Y	1.21	100	0	1.67	100	0	1.59	100	0
40	Zr	2.90	58	42	3.96	51	49	2.98	43	57
42	Mo	4.44	63	37	5.08	52	48	3.96	40	60
44	Ru	2.53	66	34	3.88	59	41	2.43	56	44
45	Rh	0.32	100	0	0.40	100	0	0.44	100	0
46	Pd	nd			0.34	0	100	0.14	0	100
47	Ag	nd								
48	Cd	nd								
50	Sn	nd								
52	Te	nd								
55	Cs	4.00	100	0	1.87	100	0	0.64	100	0
56	Ba	3.93	100	0	3.94	100	0	3.49	100	0
57	La	3.56	100	0	3.26	100	0	2.89	100	0
58	Ce	23.85	100	0	21.94	100	0	21.23	100	0
59	Pr	3.00	100	0	2.69	100	0	2.79	100	0
60	Nd	10.25	100	0	9.11	100	0	9.15	100	0
62	Sm	2.08	100	0	1.74	100	0	1.97	100	0
63	Eu	0.64	100	0	0.78	100	0	0.51	100	0
64	Gd	0.20	100	0	0.17	100	0	0.20	100	0
92	U	–	–	–	0.94	100	0	0.81	100	0

[a] nd = Not determined (the elements were in the non-ionic precipitates).

was not so large that it migrated in the terminating zone in a zone electrophoretic mode (Fig. 4).

From Fig. 5, it was expected that most of the Fe, Zr, Mo and platinum group elements were precipitated in the non-ionic fractions. Fig. 6 shows the PIXE spectrum of the red-brown precipitate. The solution of non-ionic fractions was decanted and the residue was used as the PIXE target after drying in a desiccator. Obviously from Fig. 6, the major components in the precipitate were Fr, Zr, Mo and Ru. Rh and Pd were also found in the precipitate.

Table V shows the component amounts determined by PIXE and their relative abundances; Ce was normalized as 100. In comparison with Table IV, the non-ionic abundance was much smaller than that with the WNH_4Ac–HIB system. As shown in Fig. 6, several elements (Te, Se, Ag, etc.) were found in the precipitate. These elements were not determined because the precipitate sample was not a so-called "thin target" but a "thick target", where correction of the X-ray absorption and energy down of the proton beam must be taken into account. The program PIXS did not fully support thick target analysis. However, it is obvious that the

TABLE IV

RELATIVE ABUNDANCES OF MW-2 COMPONENTS IN THE FRACTIONS (Ce = 100)

Z	Element	Relative abundance (%)			
		Sample	Sampling rate (μmol/h)		
			123	80	60
24	Cr	6.7	5.7	5.9	3.6
25	Mn	22.3	22.2	21.4	21.5
26	Fe	131.9	120.1	124.0	108.4
28	Ni	15.9	15.1	15.0	14.2
34	Se	0.9	0.0	0.0	0.0
37	Rb	6.2	4.0	2.0	0.3
38	Sr	14.9	12.3	13.3	13.0
39	Y	10.7	5.1	7.6	7.5
40	Zr	61.3	12.2	18.1	14.0
42	Mo	52.0	18.6	23.2	18.7
44	Ru	28.7	10.6	17.7	11.5
45	Rh	5.8	1.3	1.8	2.1
46	Pd	14.7	nd[a]	1.6	0.7
47	Ag	0.6	nd		
48	Cd	0.8	nd		
50	Sn	0.6	nd		
52	Te	6.1	nd		
55	Cs	27.3	16.8	8.5	3.0
56	Ba	16.5	16.5	18.0	16.4
57	La	13.9	14.9	14.9	13.6
58	Ce	100.0	100.0	100.0	100.0
59	Pr	12.7	12.6	12.3	13.1
60	Nd	42.4	43.0	41.5	43.1
62	Sm	8.7	8.7	7.9	9.3
63	Eu	1.4	2.7	3.6	2.4
64	Gd	0.7	0.8	0.8	0.9
92	U		0.0	4.3	3.8

[a] nd = Not determined (the elements were in the non-ionic precipitates).

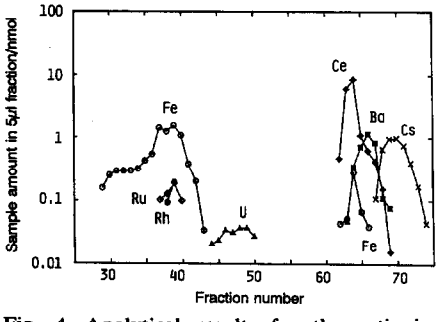

Fig. 4. Analytical results for the cationic and non-ionic fractions of MW-2 obtained by means of PIXE with the WNH_4Ac–Tar system. Molar sampling rate, 80 μmol/h; migration current = 30 mA; temperature of separation chamber = 15°C.

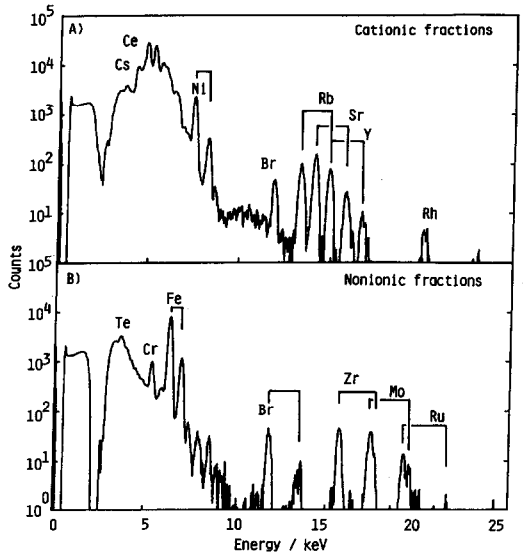

Fig. 5. Merged PIXE spectra of (A) the cationic fractions and (B) the non-ionic fractions. Electrolyte system, WNH_4Ac–Tar; $E_p = 2$ MeV.

WNH_4Ac–Tar system is suitable for fractionating platinum group elements by means of free-flow ITP.

As the electrolyte system used is two-directional, simultaneous fractionation of anions, non-ions and cations was tried using the Elphor Vap 22 instrument. However, it was unsuccessful. The width of the separation chamber (10 cm) of the present instrument seems to be too small for two-dimensional fractionation of the present model waste. Better fractionation might be

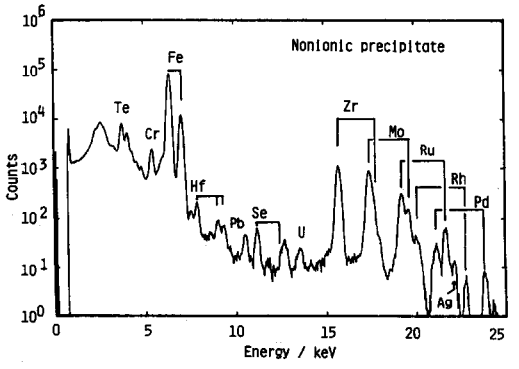

Fig. 6. PIXE spectra of the non-ionic precipitate in non-ionic fractions. Electrolyte system, WNH_4Ac–Tar; $E_p = 2$ MeV.

TABLE V

COMPONENT AMOUNTS DETERMINED BY PIXE

Electrolyte system: WNH_4Ac–Tar. T = total amount (nmol) of sample components found in 5-μl fractions; C = recovery as cations (%); N = recovery as non-ions (%).

Z	Element	T (nmol)	Relative abundance (%)	C (%)	N (%)
24	Cr	0.54	3.1	100	0
25	Mn	4.15	23.6	100	0
26	Fe	8.84	50.3	6	94
28	Ni	2.76	15.7	100	0
34	Se	nd[a]			
37	Rb	nd			
38	Sr	2.41	13.7	100	0
39	Y	1.15	6.6	100	0
40	Zr	0.56	3.2	0	100
42	Mo	0.73	4.2	0	100
44	Ru	0.20	1.1	0	100
45	Rh	0.14	0.8	100	0
46	Pd	nd			
47	Ag	nd			
48	Cd	nd			
50	Sn	nd			
52	Te	nd			
55	Cs	4.15	23.6	100	0
56	Ba	3.25	18.5	100	0
57	La	2.42	13.8	100	0
58	Ce	17.56	100.0	100	0
59	Pr	2.08	11.9	100	0
60	Nd	7.74	44.1	100	0
62	Sm	1.56	8.9	100	0
63	Eu	0.63	3.6	100	0
64	Gd	0.18	1.0	100	0
92	U	0.21	1.2	100	0

[a] nd = Not determined (the elements were found only in the non-ionic precipitates).

achieved by using a separation chamber of width 50 cm or more.

ACKNOWLEDGEMENT

The authors express their thanks to Power Reactor and Nuclear Fuel Development (Tokyo, Japan) for financial support of part of this work. T.H. also wishes to thank the Ministry of Education, Science and Culture of Japan for support of part of this work under a Grant-in-Aid for Scientific Research (No. 04650683).

REFERENCES

1 T. Hirokawa, M. Ueda, A. Ijyuin, S. Yoshida, F. Nishiyama and Y. Kiso, *J. Chromatogr.*, 633 (1993) 261.
2 F.E.P. Mikkers, F.M. Everaerts and J.A.F. Peek, *J. Chromatogr.*, 168 (1979) 293.
3 F.E.P. Mikkers, F.M. Everaerts and J.A.F. Peek, *J. Chromatogr.*, 168 (1979) 317.
4 W. Thormann, D. Arn and E. Schumacher, *Electrophoresis*, 6 (1985) 10.
5 T. Hirokawa, K. Watanabe, Y. Yokota and Y. Kiso, *J. Chromatogr.*, 633 (1993) 251.
6 T. Hirokawa, F. Nishiyama and Y. Kiso, *Nucl. Instr. Methods*, B31 (1988) 525.
7 P. Boček and F. Foret, *J. Chromatogr.*, 313 (184) 189.